INTERNAL NOTE MSC-EG-68-19

PROJECT APOLLO

DYNAMIC TESTING OF APOLLO SPACECRAFT IN THE FLIGHT ENVIRONMENT (STROKING TEST)

PREPARED BY

William H. Peters

APPROVED BY

Kenneth J. Cox
Chief, Systems Analysis Branch

Robert G. Chilton
Deputy Chief
Guidance and Control Division

NATIONAL AERONAUTICS AND SPACE ADMINISTRATION

MANNED SPACECRAFT CENTER

HOUSTON, TEXAS

DECEMBER 31, 1968

No

NATIONAL AERONAUTICS AND SPACE ADMINISTRATION

INTERNAL NOTE MSC - EG - 68 - 19

PROJECT APOLLO

DYNAMIC TESTING OF APOLLO SPACECRAFT IN THE FLIGHT ENVIRONMENT (STROKING TEST)

MANNED SPACECRAFT CENTER
HOUSTON, TEXAS

December 31, 1968

CONTENTS

INTRODUCTION

The concept of an inflight stroking test is simple, inexpensive, easy to perform, and provides significant benefit in the development of an aerospace vehicle. This internal note (1) describes the stroking test that is scheduled to be performed on Apollo (Mission D), (2) provides a justification for the test, (3) describes procedure and criteria, (4) gives an account of preflight analysis that has been performed, and (5) presents the postflight analysis plan.

Stroking Test Description

The fundamental concept associated with the stroking test is "frequency response." The frequency response of a plant, or process, to which control inputs must be applied, is perhaps the most descriptive characteristic that can be measured. This is particularly true if closed loop control is required, and conditions are such that sustained oscillations can occur. In this instance, dynamic compensation must be designed and the frequency response characteristics of the CSM/LM spacecraft becomes essential information.

A frequency response test is normally thought of in terms of a long, drawn out process, where sinusoidal test excitations are applied on a single frequency basis for numerous test frequencies. Assuming linear response of the plant, the principle of superposition may be applied to show that it is unnecessary to apply test excitation inputs on an individual basis. An additional concern of frequency response testing is the belief that one must wait for steady state conditions subsequent to applying each test input. This is true in the case of single frequency testing because the normal method of data reduction does not account for the fact that the dynamic state of the device was "at rest" when the excitation began. The principle of the stroking test is as follows:

a. Excitation is assumed to have been applied for a long time prior to, and a long time following the actual physical application of excitation.

b. The excitation is composed of an infinite number of individual test inputs, all sinusoidal and all being applied simultaneously.

c. The amplitudes and phase relationships of these test inputs are such that the net result is zero up to the point in time where the actual physical stroking begins, is exactly equal to the stroking signal during the time interval of its application, and is again zero for all time thereafter.

Choosing the amplitude and phase relationships between the individual test inputs in this manner permits an extremely short total excitation time (7.3 seconds for the Apollo test).

The Apollo test consists of commanding the SPS engine gimbal pitch actuator at a constant rate for a short period of time, reversing polarity of the drive command for another period of time, etc. to form a series of ramp inputs. The SPS engine gimbal command is shown in Figure 1. Note that it has been designed to be symmetrical so that no residual cross axis velocity remains after the test. It is generated by a subroutine in the command module computer (CMC), independent of structural response and normal controller action. It is summed with the normal controller commands to the SPS engine actuator. This particular forcing function was designed by an iterative analysis process that yielded a nearly flat power density spectra between 1.0 and 3.0 Hz, with very little energy at frequencies outside this band. It should be noted that the forcing function does not dwell at a particular input frequency for more than two seconds.

At first thought it appears that the control system would treat this input as a disturbance and thereby generate commands to try and cancel the stroker input. This is indeed the case; however, the TVC controller for LM docked, in the COLOSSUS I flight program, is designed to provide large attenuations at frequencies above 0.1 Hz. The net result is that the engine angle command is nearly identical to the stroking command. Even if the actual engine position time history should differ significantly from the stroker command (due to a guidance input, for example), the test would still be valid because SPS engine position will be telemetered so that the true airframe excitation will be known. The actual format of the excitation signal is somewhat arbitrary as long as certain constraints are met. These constraints are: (a) sufficient excitation of the significant elastic modes of interest, and (b) acceptable structural loads and crew comfort. The excitation function of Figure 1 has been shown to meet these criteria with the control and guidance loops functioning in a closed loop simulation (reference 5).

Justification for Flight Test

Reference 1 constituted the original request that this flight test be adopted. The objectives were more ambitious at that time because there was hope that triaxial, linear accelerometers could be added, and also that telemetry would be available from the docked LM vehicle. Due to tight schedules, high demand for telemetry channels, high costs for addition of measurements, etc., the additional telemetry was disallowed. Furthermore, to get telemetry from the LM during the docked SPS burn would place a constraint on the mission timeline (create a requirement for crew to go into the LM and power up sooner than this would normally be done). This left only the CSM SCS rate gyro information available as structural response data.

This data source rules out one of the prime, original justifications for the test; that of providing data to the structural analyst for calibration of the mathematical models used in the generation of bending mode shape information. In other words, bending mode shape information per se cannot be obtained from the rate gyro measurement alone. However, the dynamic gain characteristic of the structural response transfer function over a band of frequency encompassing the first two bending modes can be obtained. In addition, phase shift information can also be obtained. This data is exactly what is needed for an end-to-end flight verification of the structural dynamics model coupled with the control system (under a thrusting environment). This information will provide a measure of stability margin at the predominant structural resonances (stability margins of all structural resonances cannot be verified without additional stroking tests that would accentuate other frequency bands). Hence, the primary objective of the test is to measure the response* of the airframe, dynamically coupled to the SPS engine actuation system, in a frequency band encompassing the first two structural bending modes. This will provide a measure of the stability margins on these two modes because the frequency response of the controller at these frequencies will be well known.

It should be stressed that the in-flight dynamic response will be known (prior to execution of the stroking test) only through an analytical extrapolation of structural response obtained from the docked modal tests performed on the ground. Some dynamical effects that are treated analytically beyond the ground test data, or that are not treated in the analytical processes due to value judgements are as follows:

a. Dynamic forces of the suspension system used in the ground tests.

b. Dynamic forces of the sloshing propellants used in the ground tests.

c. Coupling paths for flow of energy into the structural resonances from the SPS engine actuator motors (tail wags dog).

d. Flow of energy from thrust force into structural resonances (dog wags tail).

These items are each discussed briefly below.

The suspension system creates small dynamic forces due to interaction with the suspension mode and due to suspension system damping forces. Due to a sizeable separation in frequency between the suspension mode and the first structural mode, these forces should be small and will probably be accounted for with sufficient accuracy.

Dynamic forces from sloshing propellants couple slightly with the structural resonances. The characteristic frequencies of the fundamental propellant sloshing modes during the ground test would be roughly double that expected in flight (LM docked case). This effect is very difficult to account for in an exact manner analytically and may not be done as a

---

* Note that "response," as used here, implies total time domain response at a particular structural point and not total time response at all structural points.

result of a value judgment ruling in favor of accepting the uncertainty as opposed to the additional effort and time required to compensate for this effect in the analysis.

Item (c) consists of two parts. The first part is the first order effects that are believed to be properly treated in the analytical models. This includes application of the engine inertial torques created by addition of an actuator length degree of freedom. The second part, believed to be of second order importance, is not treated by the existing analytical models. This includes a forcing of the bending modes through the compliance of the actuator attach points, and a coupling with the torsional modes due to actuator motor reaction forces.

Analysis indicates that item (d) will cause a significant reduction in the damping of the first bending mode. For what is believed to be a severe combination of tolerances on both the structural mode data and actuator parameters the first bending mode damping can be driven negative.

It is felt that there are real potential sources of error in the analytical predictions of the in-flight dynamic response, even though there may exist high confidence in the quality of the structural bending mode data. The in-flight stroking test is felt to be highly justified in order to provide flight validation of these effects.

Figure 2 shows the logic flow for integrating structural dynamics data into the overall powered flight control system design and development process. It should be noted that the in-flight stroking test fills a basic need in the control system design verification. Additional discussion pertinent to the overall justification for the test appears in the section on tradeoffs regarding risk.

Mission and Program Impact

The primary mission requirement for performance of the stroking test is a relatively long, CSM/LM, SPS engine burn. This created a small mission planning impact for the once planned 207/208 mission, but fortunately, original planning for a D type mission using a Saturn V booster had two long, out-of-plane, SPS engine burns. This provides the ideal situation for performance of the stroking test. It allows ample time for an initial test at reduced amplitude, real time safety evaluation, test amplitude change; and one final test, all without significant impact on crew timeline. The detailed test procedure and inherent risks involved, both with and without the stroking test, are discussed below.

Flight Test Procedures

The stroking test is performed in a completely automatic mode, with the exception that it must be manually enabled by execution of verb 68 ENTER via DSKY. If this verb is executed at any time other than during a TVC DAP controlled SPS burn, the operator error alarm light is activated and control is returned to the program previously being executed (reference 2). If the stroke test is enabled after T_{IG} but prior to T_{IG} + 10 seconds, the excitation will begin at T_{IG} + 10 seconds. When the test is enabled after T_{IG} + 10 seconds, the excitation begins immediately.

The excitation function terminates automatically 7.3 seconds after it begins, but the requirement for test data stipulates that the burn must continue for several seconds beyond that point. The exact amount of burn time required beyond the end of test excitation is a function of the following parameters:

a. Test excitation amplitude
b. Telemetry threshold
c. Structural response characteristics
d. Requirement for information quality

Since item (d) is somewhat subjective in nature and item (c) is not well known, there is no exact time requirement for data. Once models are assumed for the first three items, however, it can be shown that the quality of the information that is derived from the data improves with the length of the data gathering interval, to a point, and then degrades for longer intervals. This requirement for length of the data gathering interval is discussed in more detail in the post-flight analysis section of this report. Analysis has shown that a burn time between 20 and 30 seconds beyond termination of test excitation is required for Apollo.

The detailed test objective for Mission D (reference 3) states that the test should be initiated at least 34 seconds prior to the end of the burn. This assures ample time for data gathering prior to thrust termination.

The flight procedure that has been established performed the stroking test in two basic parts. The first time the test excitation function is activated it produces the desired waveform but all amplitudes are scaled at 40 percent of the required nominal amplitude. If it is then judged by the crew and ground controllers that a full amplitude run is safe, a single constant in erasable memory (ESTROKER at location 03001) is changed from 00002_8 to 00005_8 and the test is repeated on the next SPS burn. This procedure lends confidence to the safety of the test, but according to data to be published in references 4 and 5, it would be perfectly safe to cycle through once at full amplitude. Also, as another possible flight procedure variant, it would be acceptable to perform both the 40 percent amplitude and full amplitude passes in the same burn, provided that at least 40 seconds is allowed to elapse between initiation of the first and final passes.

The recommended criteria for judging safety of the full amplitude pass is that the SCS rate gyro output oscillations during the reduced amplitude pass not exceed 0.8 degrees per second peak to peak. This implies that the 1.0 degree/second scale should be selected on the FDAI. In the event that a premature termination of the excitation is desired, a forced computer restart using verb 69 may be employed. An alternate procedure would be to switch to SCS control.

The criteria for test abort is 0.8 degree/second peak to peak during the reduced amplitude test, or 2.0 degree/second peak to peak for the full amplitude test. Structural loads at the docking interface for the latter are predicted to be on the order of 100,000 inch pounds in bending, 7,000 pounds in compression, and less than 20,000 inch pounds in torsion. This should provide a safety factor greater than four.

Tradeoff Regarding Risk

The impact this test has on the "D" mission timeline and crew activity timeline is quite small. The remaining question is: "What is the risk involved for not performing the test as opposed to the risk involved in performance of the test?" This question could have been considered in the section on justification, but it is best considered after the reader has been acquainted with the flight test procedure.

First of all, it should be established that there is a certain element of risk that the attitude control system will be unstable when the SPS engine is first ignited for the first burn on mission "D". Every reasonable effort has been made to assure that this will not occur, but there is still that small probability that something may have been erroneously judged significant or not even thought of in the analytical process. Without the stroking test, this small probability that an instability will occur grows with burn time on this and each succeeding mission.

Assuming now that the stroking test has been performed and reasonable stability margins have been validated, the probability of a powered flight control system instability for future flights is essentially zero. Furthermore, it should be emphasized that performance of the test itself in no way affects the probability of instability on Mission D if linear response is assumed. Hence, performance of the stroking test "trades off" the small probability of a future powered flight instability for an also small probability of crew discomfort and/or structural damage due to the stroking test alone.

Since both of these contingencies are remote and functions of variables too numerous to mention, it is impractical to compute realistic probability data for comparison purposes. However, with extensive preflight analysis and testing (see below) and also a prudent flight test procedure (as described above), it is expected that the former would far outweigh the latter.

Test Preparation

The first section below briefly summarizes the work that has been accomplished in the areas of: (a) design of the test excitation signal,

(b) demonstration of the validity of the analysis technique, (c) investigation of data requirements, (d) stroker program software verification, (e) structural loads computations, and (f) hardware tests. A post flight analysis plan is then presented.

Preflight Analysis and Simulation

References 4 through 12 are a partial bibliography of memoranda and reports that either address the stroking test directly or contain material pertinent to one of the subjects mentioned above. No attempt will be made here to repeat all of the material contained therein, but selected figures are borrowed and each reference summarized briefly below.

Reference 6 presents the final signal design that evolved after the decision was made to use a near flat power density spectrum, and the software program constraints were taken into account. Data presented in this report also demonstrated the effectiveness of the analysis techniques to be employed, by operating on the simulated vehicle time response to generate a transfer function from time domain data. The exercise was repeated for assumed data gathering intervals of 27 and 57 seconds. Assuming that noise due to non-zero initial conditions and imperfections in data retrieval were nonexistent, the amplitude ratio error for 57 seconds of data was 1.5 db, while that for 27 seconds of data was 5.5 db.

Reference 7 presents data showing the effects of telemetry quantization and telemetry channel saturation on the ability to reconstruct the airframe transfer function. The telemetered data is transmitted via an eight-bit binary word which breaks the dynamic range of the measurement channel into 256 parts. For the Apollo block II spacecraft the rate gyro data is monitored "downstream" from the FDAI rate scale selector switch. This means that dynamic range on the rate information is either 10.0 degrees per second or 2.0 degrees per second, depending on whether the ± 5 or the ± 1 rate scales are chosen by the astronaut. This gives rate data quantization into increments of 0.0376 and 0.0075 degrees per second respectively.

Hence, less high frequency quantization noise is present if the smaller scale is chosen, but then there is a small risk that the rates may exceed 1.0 degrees per second during the test and information would be lost. Reference 7 shows the effects of these two data coarseness levels and also results for "clipping" as much as 20 percent at peak amplitudes (i.e., running the gyro response data through a limiter with limit value set at 80 percent of the peak response).

The essential conclusions of this study were that neither the data quantization nor channel saturation would seriously degrade the capability to construct the amplitude ratio by more than 2.5 db at the resonant peaks of the first two structural bending modes. The phase data was affected very little by the quantization of 0.0075 degrees per second (± 1.0 scale) or by the 20 percent data clipping, but was degraded significantly by the rate quantization of 0.0376 degrees per second (the ±5.0 scale). This would imply that the ±1.0 rate scale should be used.

Reference 8 shows the effect of the FDAI display dynamics on the rate information. The indicator dynamics attenuate the rate information such that peak amplitudes observed on the FDAI rate needles will be approximately 20 percent less than actual. Fortunately, the bulk of this "filtering" is downstream from the telemetry pickoff such that the telemetered data quality is not impaired.

Reference 9 documents the minutes of a meeting held to review the stroking test justification and the structural loads situation. North American Rockwell (NR) had expressed concern that torsional loads in the docking tunnel resulting from the stroking test were excessive. The MSC structural people did not concur with this position. An elaborate simulation at NR (references 5 and 11) and a stroking test simulation during the docked modal survey structural ground test (references 4 and 10) have since substantiated this position.

Figure 3 presents time response data from the simulator at NR described in reference 4. This simulation used a real flight type hardware computer, actual flight program (SUNDISK 282), hardware SPS engine actuator, coupling data units (CDU's) and display and keyboard (DSKY). Eleven bending modes were used in what is thought to be a reasonably accurate flexible body dynamics model, and a reasonably accurate loads transformation was used. The stroking test was initiated via verb 68 through the DSKY. The peak torsional loads indicated are roughly one third the expected tolerable level.

In addition, reference 4 (to be published) is expected to independently substantiate the fact that structural loads due to the nominal stroking amplitude are well within tolerable levels.

Post Flight Analysis Plan

The test description section of this report discusses the background theory related to this test in general terms. References 13, 14, and 15 are recommended as good material on some of the broader aspects or relevant details. The output of a linear system y(t) can be obtained by summing all past unit impulse responses $h(t-\tau)$, weighted by the value of the input function at time $t = \tau$, $x(\tau)$. Stated symbolically

$$y(t) = \int_{-\infty}^{t} x(\tau)h(t-\tau)d\tau \qquad (1)$$

In the limit, as $t \rightarrow \infty$, the Fourier transform of y(t) can be expressed as the product of the Fourier transforms of x(t) and h(t), i.e., if

$$\begin{aligned} F\{y(t)\} &= Y(jw) \\ F\{x(t)\} &= X(jw) \\ F\{h(t)\} &= H(jw) \end{aligned} \qquad (2)$$

then

$$Y(jw) = X(jw)H(jw) \tag{3}$$

Let $x(t)$ be the telemetered stroking function (excitation) and $y(t)$ be the telemetered vehicle response function. Then, by processing these time response functions to obtain their Fourier transforms, $X(jw)$ and $Y(jw)$ respectively, we have

$$H(jw) = \frac{Y(jw)}{X(jw)} \tag{4}$$

Equation (4) is a theoretical result and not completely attainable in practice due to the following reasons:

a. Exact analytical expressions for the two time functions are not available.

b. Telemetry thresholds and other effects add noise to the accumulated data.

c. Numerical techniques for computing the Fourier transforms have limitations to the dynamic range and accuracy problems due to time quantization of the data.

As a result, equation (4) will be valid only for certain intervals of w. This can be explained huristically as those frequency intervals where the response data is reasonably representative of the true system response to the input.

For the Apollo Mission D stroking test, the excitation has been designed to provide a large amount of excitation in the range between 1.0 and 3.0 Hz, but very little elsewhere. Hence, for those characteristic dynamics in this frequency band that have significant contributions to the measured response, equation (4) will be valid. The process has been demonstrated using the response of an analytical model of the Apollo spacecraft as discussed in the preceding section.

The "plan" for post flight data reduction is as follows:

a. Obtain the following time history data from telemetry data:

(1) SCS Body Rate Pitch (CH3503R)
(2) SCS Body Rate Yaw (CH3504R)
(3) SCS Body Rate Roll (CH3505R)
(4) TVC Pitch differential current (CH3666C)
(5) SPS Engine Gimbal Position Cmd., Pitch (*)
(6) SPS Engine Gimbal Position Cmd., Yaw (*)
(7) SPS Engine Gimbal Position Pitch (CH3517H)
(8) SPS Engine Gimbal Position Yaw (CH3518H)
(9) Yaw channel guidance command (*)
(10) Roll control torques from the RCS (CH3554X through CH3561X)

*Constructed from downlist data (CG001V) and knowledge of software programs.

b. Obtain Fourier transforms for each time function, assuming the value of the functions to be identically zero for all time preceding initiation of test excitation, and for all time after approximately 40 seconds.

c. Compute amplitude ratio and phase shift information as a function of frequency for the following transfer functions:

(1) CH3503R/Pitch Gimbal Posn. Cmd.
(2) CH3504R/Pitch Gimbal Posn. Cmd.
(3) CH3505R/Pitch Gimbal Posn. Cmd.
(4) CH3518H/CH3517H
(5) CH3503R/CH3517H
(6) CH3517H/Pitch Gimbal Posn. Cmd.

d. Construct power density spectra plots for the TVC pitch differential current (CH3666C), roll control torques from the RCS, and the yaw channel guidance commands.

e. Compare data from item c(1) with analytically predicted response using structural data from the ground test. Differences in these data can be used to establish new control system stability margins. If the differences are small, then there is high probability that the analytical models treat all significant dynamic coupling effects with sufficient fidelity and depth. If the differences are gross, then either the analytical models are inadequate or the data quality (and quantity) is too low to provide conclusive answers.

f. Items c(2) and c(3) represent the crosscoupling from pitch control into yaw and roll control through the structural dynamics. This will be meaningful data only if yaw and roll excitation from other sources is small in the frequency band where stroking occurs. This is determined from item d.

g. Item c(4) is a measure of the net crosscoupling into yaw control and expected to be small compared to item f due to large attenuation in the yaw control filter.

h. Item c(5) may provide a calibration point with the structural ground test data. If there is good agreement between the amplitude ratio and phase information of this data in comparison with that published in reference 4, then there is high probability that the potentially significant effects discussed earlier are of little consequence. On the other hand, a significant disagreement may mean simply that the "tail-wags-dog" effects are large. This cannot be established exactly, but an attempt can be made to bring item c(5) data into agreement with the ground test data by compensating for the tail-wags-dog effects as follows:

(1) Construct an analytical airframe model that can be forced by clutch current (CH3666C) only through the resulting engine inertial forces.

(2) Subtract this time function from CH3503R and recompute item c(5).

Good agreement after the above manipulations would constitute additional verification of the analytical models used for control system design.

i. Item c(6) will yield the transfer function of the coupled actuator and provide information on the extent of the dynamic coupling of the actuator with the airframe through the "dog-wags-tail" effect.

j. Item d provides information on potential obscuration of data due to inputs other than the intended test excitation. Pitch rate gyro response due to yaw guidance commands and roll torques, for example, would be computed from an analytical model and compared with measurement CH3503R. In the event that this exercise should indicate that CH3503R data is significantly affected by these excitation sources, then an attempt would be made to compensate for these inputs by subtracting out their estimated contributions.

Concluding Remarks

a. The stroking test planned for Apollo Mission D has been described in detail. This information should be useful to those involved in scheduling and performing the test in the flight environment.

b. Preflight analyses and tests have been performed which demonstrate soundness of the basic approach and safety of the test.

c. Test excitation may be terminated prematurely via verb 69 E through the DSKY or by switching to SCS control.

d. A post flight analysis plan has been presented.

References

1. Memorandum EG23-132-65-906, "In-flight stroking tests for Apollo," October 21, 1966

2. Lockheed Electronics memorandum LEC/GC/56, "Stroking Test," July 26, 1968.

3. Mission Requirements, "D" Type Mission, LM Evaluation and Combined Operations, DTO 1.23.

4. SMD's report on ground stroke test (to be published).

5. NR's report on HE simulation results (to be published).

6. Lockheed Electronics report, "Reconstruction of Apollo Spacecraft Transfer Function and Test Signal Design," ED Project 1122, January 16, 1967.

7. Memorandum EG23-67-139, "Effects of telemetry quantization and channel saturation on stroking test data validity," August 15, 1967.

8. Memorandum EG23-67-232, "FDAI attitude rate display of stroking test response," December 12, 1967.

9. Memorandum EG2-M-12-67-970, "Mission D stroking test," October 27, 1967.

10. NASA Technical Report, "Engineering Test Requirements for CSM LM Docked Modal Survey," May 1968.

11. Memorandum EG23-68-11, "Recommended Test Matrix for Block II DAP Evaluation at NR," January 16, 1968.

12. Memorandum EG23-138-68-778, "Summary of TVC DAP Technical Interchange Meeting, July 12, 1968.

13. Lee, Y. W., Statistical Theory of Communications," John Wiley and Sons, Inc., 1961.

14. Weiner, Norbert, "The Fourier Integral and Certain of its Applications," Dover Publications, Inc., New York, 1933.

15. Truxall, John G., <u>Control System Synthesis</u>, McGraw Hill, 1955.

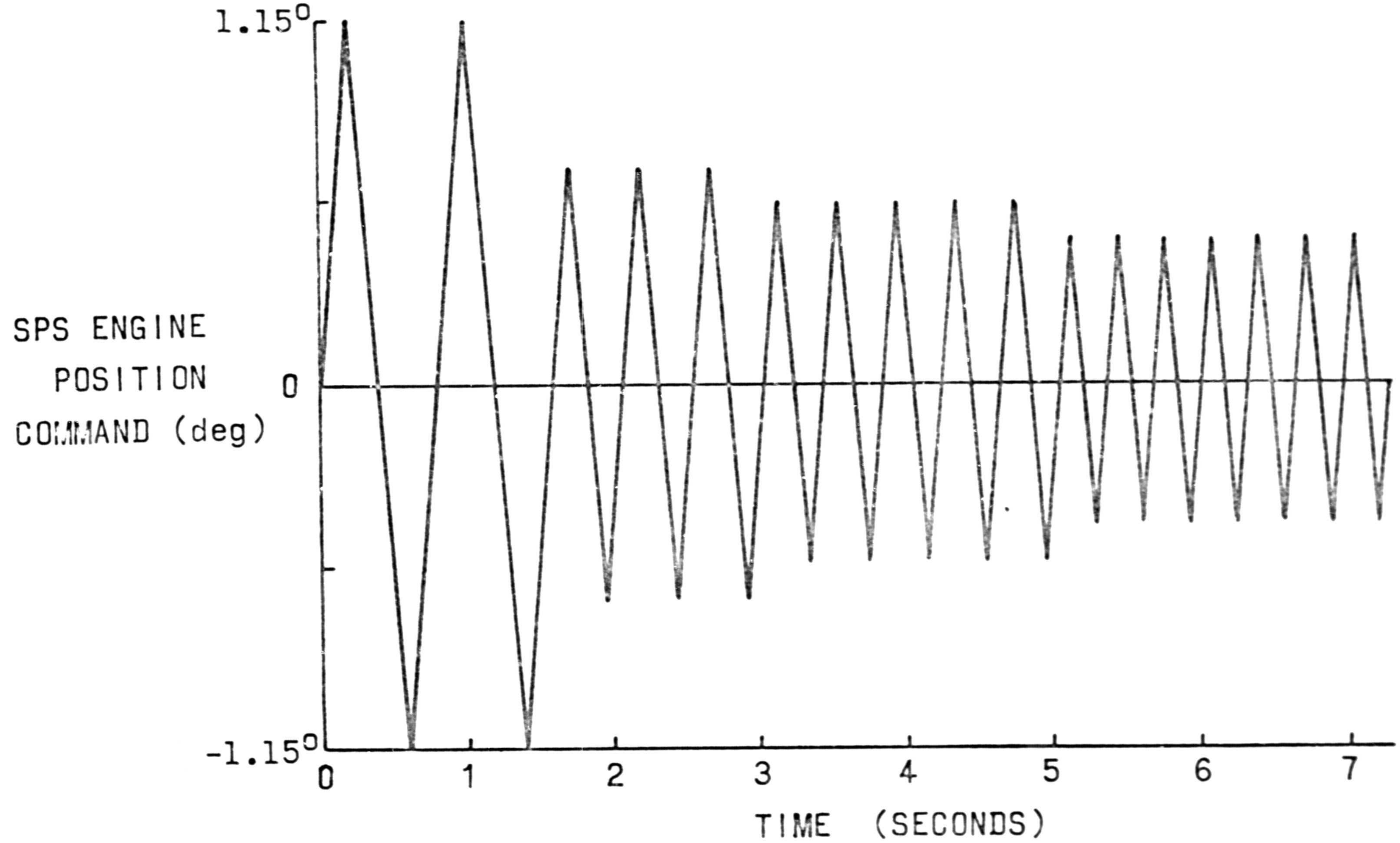

Figure 1. - Stroke testing excitation function

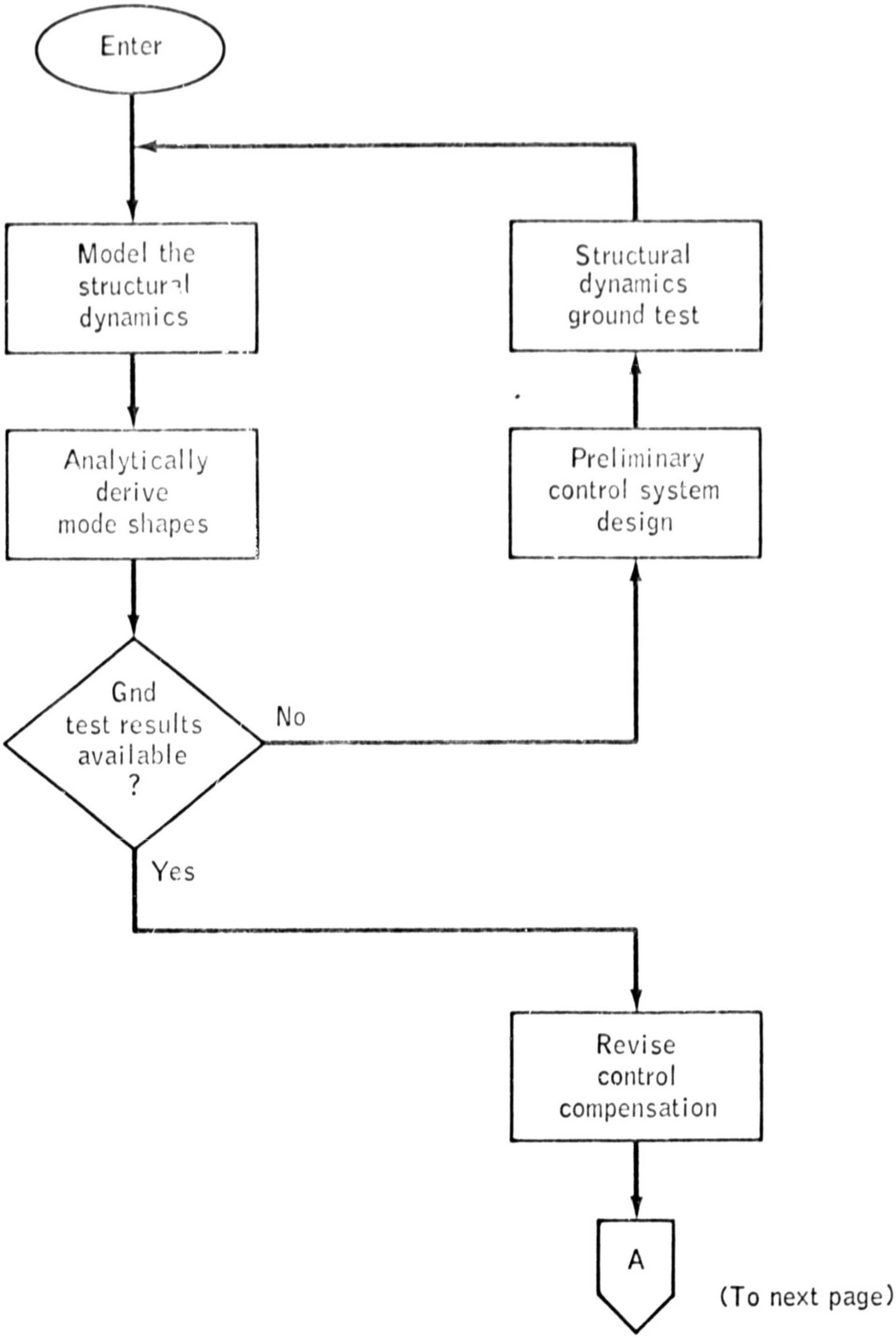

Figure 2. - Relationship of the structural ground test and stroking test to control system development process.

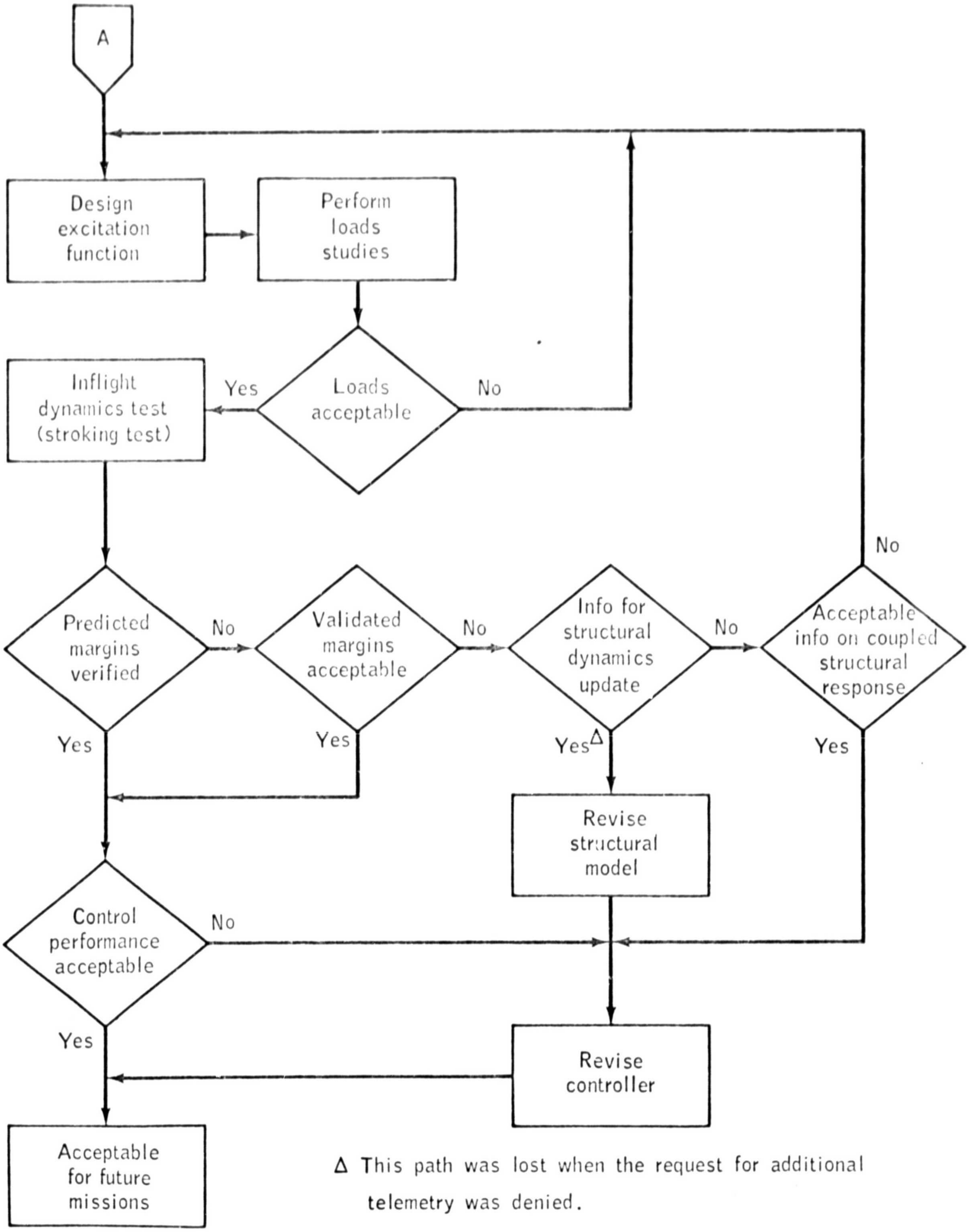

∆ This path was lost when the request for additional telemetry was denied.

Figure 2. - Concluded.

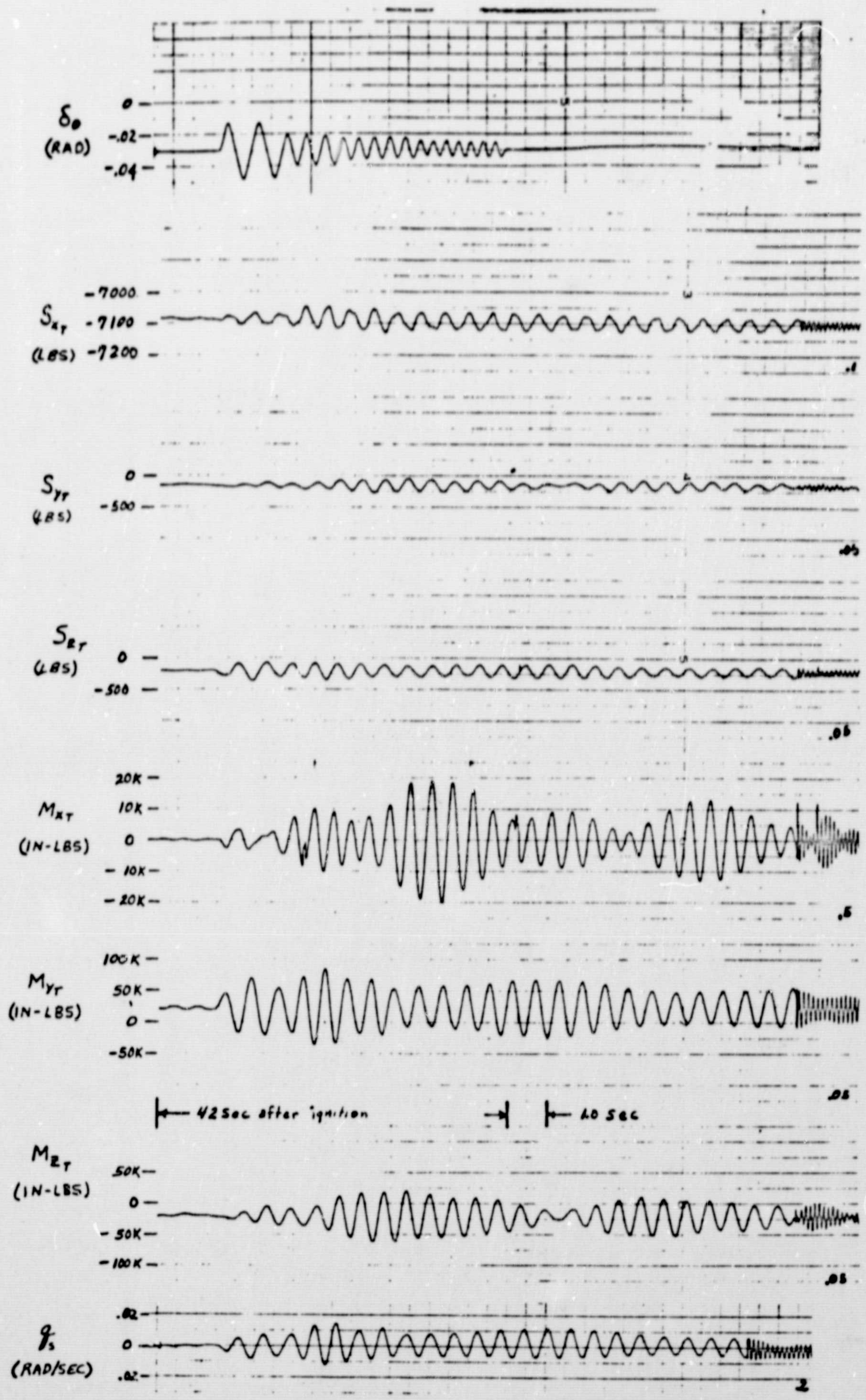

Figure 3. - Docking tunnel load response to stroking test CSM-LM DAP, TRW bending data.